(Received 7 August 2024, Accepted 14 October 2024, Scheduled 21 October 2024)

Research on Ultra Narrow Size Microstrip Multiband Antenna Suitable for Wireless Repeaters in Mine Tunnels with Different Cross-Sections

Yun Li[1,2], Peng Chen[3,*], and Bo Yin[3]

[1]Chongqing Research Institute, China Coal Technology & Engineering Group, Chongqing, China
[2]State Key Laboratory of Coal Mine Disaster Prevention and Control, Chongqing, China
[3]School of Optoelectronic Engineering, Chongqing University of Posts and Telecommunications, Chongqing, China

ABSTRACT: Through the analysis of experimental data, it is found that the optimal communication frequencies of mine tunnels with different cross-sections are different. These optimal operating frequency bands (580–600 MHz, 806–826 MHz, 1427.9–1447.9 MHz, 2401.5–2481.5 MHz, 5150–5600 MHz) are not only numerous, but also wide-ranging. Meanwhile, because the wireless repeater in the mine tunnel has great restrictions on the antenna size, the antenna has to be designed in a very small range of transverse size. In this paper, an ultra-narrow sized multi-frequency dipole ($0.41\lambda \times 0.04\lambda$) is proposed to cover the optimal communication bands of underground mine tunnels with different cross-sections. This multibranch dipole consists of three main parts: lateral long branch, middle short branch, and end-loaded reverse branch. By adjusting the length of the two lateral long branches and utilizing high harmonics, the antenna covers the lowest and highest operating bands that differ by a factor of seven. The middle short branch is one of the contributors to 1.4 GHz band. Meanwhile, the performance of the antenna at high frequencies is optimized by adjusting the distance between branches. The bandwidth of 1.4 GHz band is expanded by the loaded reverse branches. The test results are in good agreement with the simulation data, and the antenna covers all the optimal communication frequencies of underground mine tunnels with different cross-sections. Its peak gain at the resonance point is greater than 0 dBi, and the structure is simple.

1. INTRODUCTION

Advances in communications technology have created the conditions for automated and efficient production. With the continuous iteration of communication systems, the underground mining industry is gradually moving towards intelligence [1, 2]. In an intelligent mine, a large amount of data such as video, voice, sensing, and control [3] needs to be interacted with in real time, and there is an urgent need for a highly reliable, high-speed, and low-latency communication network [4]. However, the mine environment presents unique challenges: limited space, rough walls, and waveguide properties of consumable media that interfere with electromagnetic waves. These factors create unfavorable conditions for building intelligent systems in mines.

Underground mine tunnel communication itself is a topic that needs to be addressed by intelligent systems [5, 6]. According to experiments, it is known that in a complete underground mine environment, the optimal communication frequencies are not the same for different tunnels. These frequencies are related to the structure, cross sectional dimensions, equipment, and other factors of the tunnel [7]. The performance of the designed single-band antenna tends to be more affected when it is transferred between different lanes, which hinders the underground communication system. Therefore, multi-band antennas are a better solution to adapt to the frequency selectivity of the tunnel.

There are many multi-frequency schemes for antennas, but their operating bands are concentrated in 2–6 GHz. Dong et al. have improved the radiating structure so that the antenna covers 5G NR/4G/WiFi/WiMAX bands, which is able to satisfy the multiple communication needs in the mine environment [8]. For coal mine application, Xu et al. have designed three microstrip antennas. Each antenna is compatible with WiMAX, WiFi, 4G and 5G NR bands [9]. Based on the effect of the Complementary Split Ring Resonator (CSRR) on the antenna performance, the antenna is designed to operate in the 2.4 GHz, 2.9 GHz, and 5.8 GHz frequency bands for WLAN applications [10]. In [11], antennas consisting of four identically shaped electrical panels cover four bands: 1.86–1.92 GHz, 2.30–2.65 GHz, 3.40–3.80 GHz, and 5.30–5.92 GHz. It can be found from publicly available literature that relatively little research has been done on antennas with more than a five-fold difference between the lowest and highest resonance frequencies. In addition, 0.5–1 GHz is an important frequency band for mining purposes as part of emergency communication systems, and antennas operating in this frequency band are crucial for rescue and disaster relief.

Meanwhile, in multiband antenna design, ultra-narrow transverse antenna size makes it very difficult to balance low frequency and high frequency performance. A monopole antenna

* Corresponding author: Peng Chen (3302435403@qq.com).

with dimensions of 261 mm × 30 mm has a bandwidth of 460–870 MHz, but its high frequency performance is missing [12]. In [13], the designed planar sleeve antenna is compact and small in size with a bandwidth (VSWR $\leq$ 3) of 810–3560 MHz. The minimum operating frequency of the antenna differs from the maximum operating frequency by a factor of 3. From these studies, it was found that the main difficulties in designing multiband antennas with restricted dimensions and widely differing operating bands are mainly twofold. First, the interplay of multiple radiating sections in a narrow size gives the antenna a chain effect across bands, which makes it difficult to adjust the antenna performance of a single frequency band individually. Antennas with narrow dimensions excite much fewer modes than those with normal dimensions. So the target operating frequency and bandwidth of the antenna are thus affected.

In addition to this, to optimize the performance of the wireless communication system under the mine, some scholars have analyzed the electromagnetic propagation characteristics of the mine environment by establishing a channel model. In [14], Song et al. propose the RT-FDTD method by combining Ray Tracing (RT) method and Finite-Difference Time-Domain (FDTD) method. It improves the efficiency and accuracy of underground mine simulation. After modeling the delay of the mine wireless channel, Song et al. analyzed the effects of tunnel size, carrier frequency, antenna position, and antenna polarization on the delay extension of the wireless channel [15]. The coverage capability of antennas in mines can be improved by optimizing the deployment of antennas [16–18].

Considering the conclusions of the above literature and combining with our experimental data, a multi-frequency scheme that can satisfy the demand of underground mine tunnel is at 580–600 MHz, 810–840 MHz, 1410–1440 MHz, 2400.5–2512 MHz, and 5115–5600 MHz [19, 20]. On the basis of the above work, this paper proposes a multi-branched dipole antenna. The antenna is mainly composed of three parts. First, through the reasonable layout of the long branch, the antenna covers four target frequency bands with a ten fold high to low frequency ratio. These two slender branches serve as resonant paths and are dedicated to the resonant frequencies of 0.6 GHz and 0.8 GHz. At the same time, the high harmonics of the long branches are utilized to cover the 2.4 and 5.4 GHz bands. This design simplifies the antenna structure and avoids excessive coupling. Then, the two short branches in the middle provide the antenna with the 1.4 GHz band. At the same time, the bandwidth of the antenna at 5.4 GHz is extended by adjusting the distance between these two short branches of similar length. Finally, to expand the bandwidth of the antenna at 1.4 GHz, a reverse branch is loaded at the end of the longest branch. This branch obtains energy through coupling with the long branch, but does not affect the other bands of the antenna.

2. ANTENNA DESIGN

2.1. Dipole Design

Multi-branching is a common method for designing multiband antennas. The target bands are complex. Not only are there many bands, but also the span of the 5 bands is large. The highest frequency point (5.6 GHz) is nearly ten times higher than the lowest frequency point (0.58 GHz). Therefore, in order to minimize the number of branches, the antenna utilizes high-order harmonic technology to achieve the target high frequency. Based on the distribution patterns of these five frequency bands, the high frequency bands of the antenna (2.4 GHz, 5.4 GHz) can be realized by multiplexing the same branches.

Due to 2.4 GHz being a higher harmonic of 0.8 GHz and 5.4 GHz being higher harmonics of 0.6 and 0.8 GHz, the four frequency bands of 0.6, 0.8, 2.4, and 5.4 GHz can be achieved with at least two branches. This provides more design space for the 1.4 GHz frequency band. At the same time, the simple structure also makes the antenna's coupling effect less obvious, which is the basis for the antenna to further optimize the bandwidth.

The length of the antenna's branches should be between the guiding wavelength in the medium and the wavelength in free space. When $f_0 = 0.59$ GHz, $l_{0.59}$ takes the value range of 59.6–125 mm; when $f_0 = 0.82$ GHz, $l_{0.82}$ takes the value range of 44.7–93.8 mm; when $f_0 = 1.43$ GHz, $l_{1.43}$ takes the value range of 25.6–53.6 mm.

Based on the above theory, a dipole with three branches at normal size is designed. As shown in Figure 1(a), the dimensions of Ant. 1 are 210 mm × 41 mm, and its dielectric substrate material is FR4 with a height of 0.8 mm.

Ant. 1 covers the first four target bands. The effect of the two branch lengths on the S-parameters of the antenna is shown in Figure 2. With the increase of $L1'$, the bands of 0.6 GHz and 1.8 GHz of the antenna are shifted to the left. Similarly, the bands of 0.8 GHz and 2.4 GHz are shifted to the left with the increase of $L2'$, and both are controlled by the same branch. After parameter optimization, the final $L1'$ is 97 mm, and $L2'$ is 80 mm.

As shown in Figure 1(b), in order to continue to optimize the antenna performance, a branch is added to Ant. 1 to become Ant. 2. The added branch is located in the middle, and it has the same length as the original middle branch. After the adjustment, the antenna's branch spacing is decreased.

As shown in Figure 3, the number of branches is also an important influence on the antenna performance. At a fixed size, the more branches the antenna has, the smaller the distance is between the branches. And the distance will change the coupling between the branches, which in turn affects the antenna bandwidth. Ant. 2 has a branch spacing of 4.2 mm, which is smaller than the spacing found in Ant. 1. Ant. 2 has better bandwidth performance than Ant. 1 at the 1.4 GHz band.

The number of branches also affects the excitation of high harmonics. As shown in Figures 4(a) and (c), Ant. 2 has a bandwidth of 5–5.41 GHz, while Ant. 1 has poor bandwidth performance. The excitable modes of these two antennas are analyzed in Figures 4(b) and (d). At normal size, both antennas have multiple modes within 5–6 GHz. For Ant. 1, 7 of the 8 modes have an model significance (MS) value of more than 0.707, but Ant. 1 has a poor bandwidth. For Ant. 2, there are only 6 of the 8 modes with an MS value of more than 0.707, but the bandwidth performance of Ant. 2 is better than that of Ant. 1 (5–6 GHz). While both antennas have the potential to

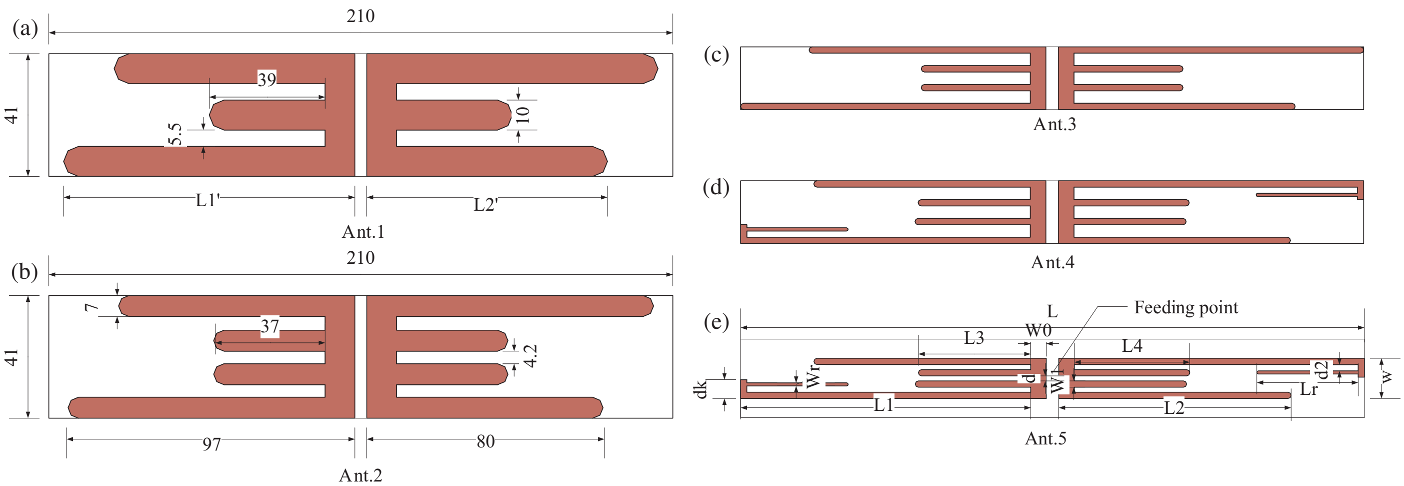

FIGURE 1. Antenna design.

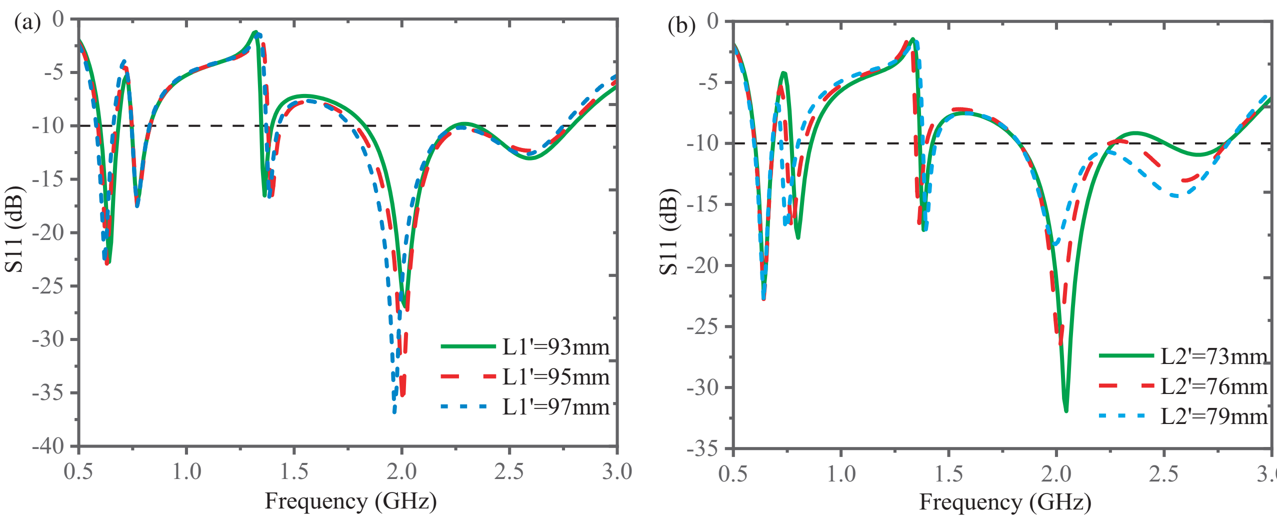

FIGURE 2. Effect of $L1'$ and $L2'$ on antenna S-parameters.

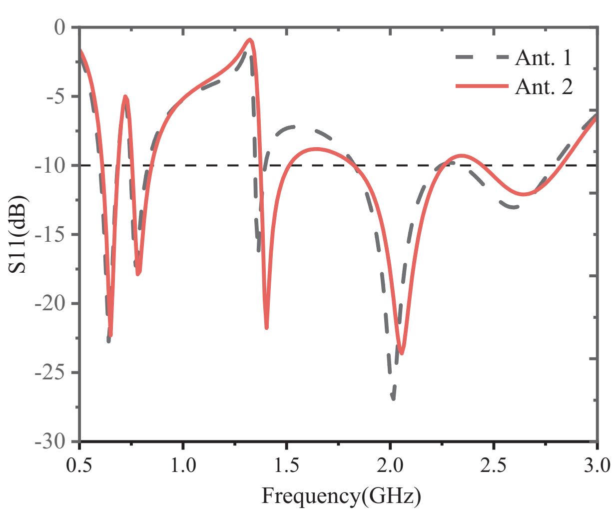

FIGURE 3. Effect of number of branches on S-parameters.

achieve multiband and wideband, there are other factors that determine whether these modes are capable of excitation. In particular, the difference between the two antennas is the distance between the branches. Therefore, the distance between branches is a key factor in exciting the high harmonics of the antenna.

2.2. Ultra-Narrow Dipole Design

The wireless repeater used in underground mine tunnel requires that the width of the antenna is not more than 20 mm. Therefore, based on the above work, the antenna size is adjusted to the corresponding range. As shown in Figures 1(c)–(e), the design of a narrowly sized dipole has three processes: Ant. 3, 4, and 5.

As shown in Figure 1(c), the antenna size was adjusted to meet the required range. The transverse dimensions of antenna 3 are 20 mm. Compared to antenna 2, antenna 3 is reduced by about 51.2%. Its frequency band is shown in Figure 5. When Ant. 2 narrows in size and becomes Ant. 3, its bandwidth performance at 0.6 GHz, 0.8 GHz, 1.4 GHz, and 2.4 GHz deteri-

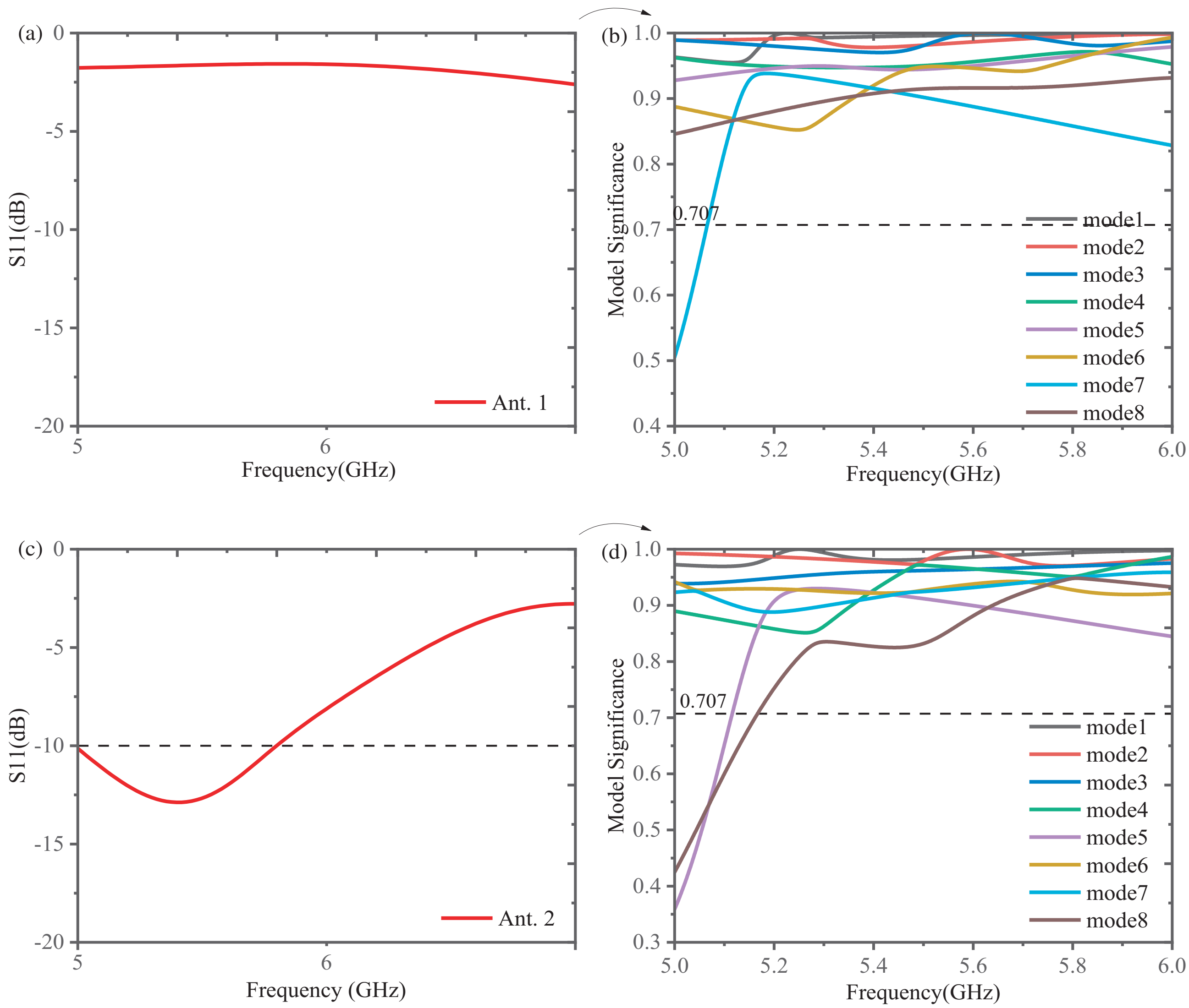

FIGURE 4. Antenna bandwidth and mode analysis (5–6 GHz).

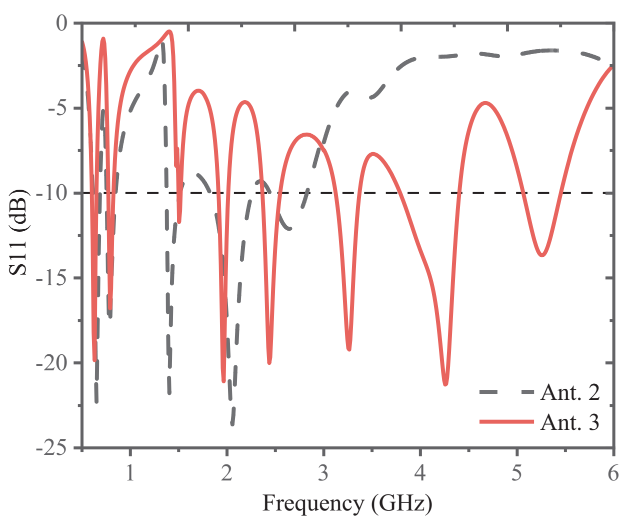

FIGURE 5. S-parameters of Ant. 2 and Ant. 3.

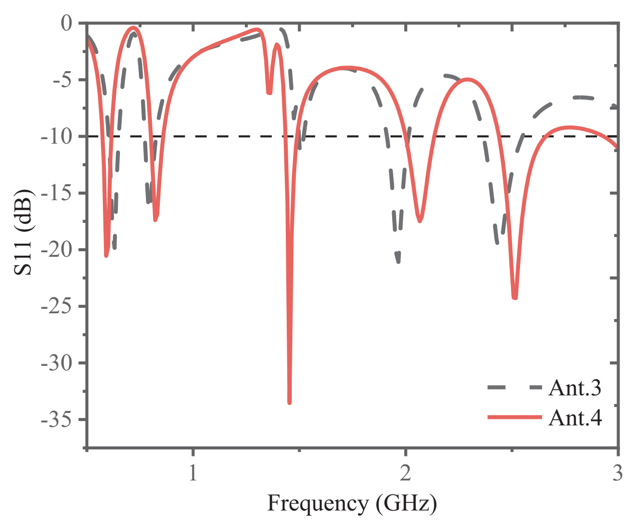

FIGURE 6. S-parameters of Ant. 3 and Ant. 4.

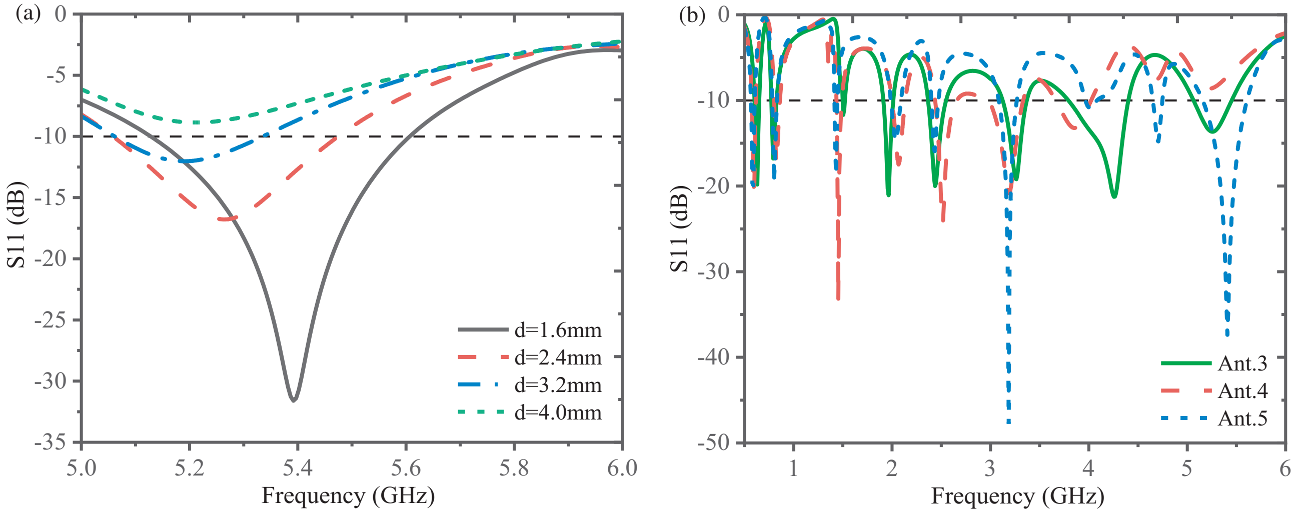

FIGURE 7. (a) Effect of spacing d on Ant. 4. (b) Bandwidths of Ants. 3, 4, and 5.

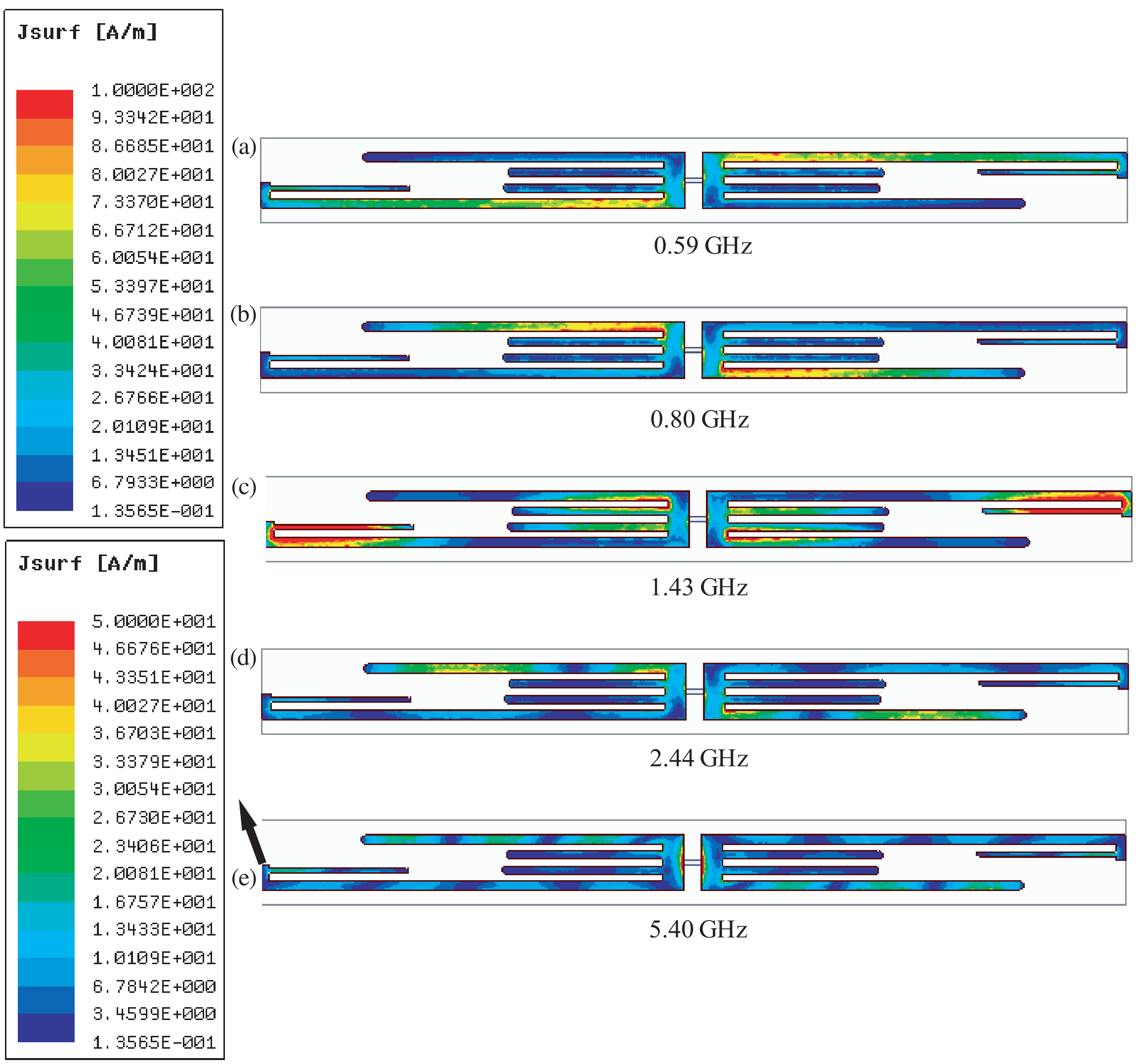

FIGURE 8. Current strength of antenna 4 at each resonance point.

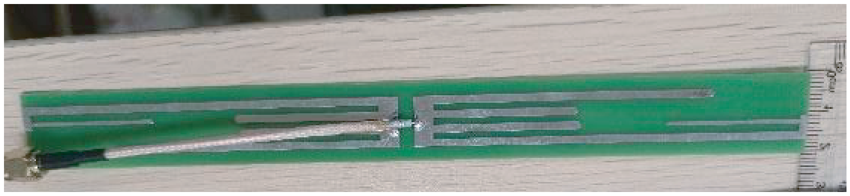

FIGURE 9. Antenna prototype.

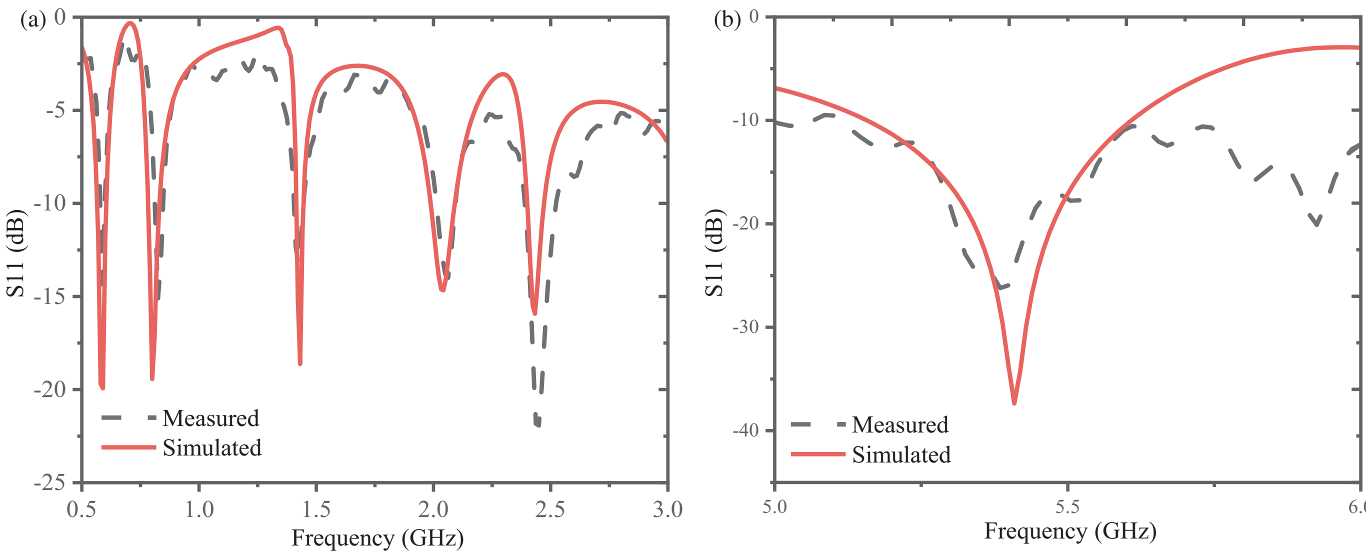

FIGURE 10. Antenna simulation and test S-parameters.

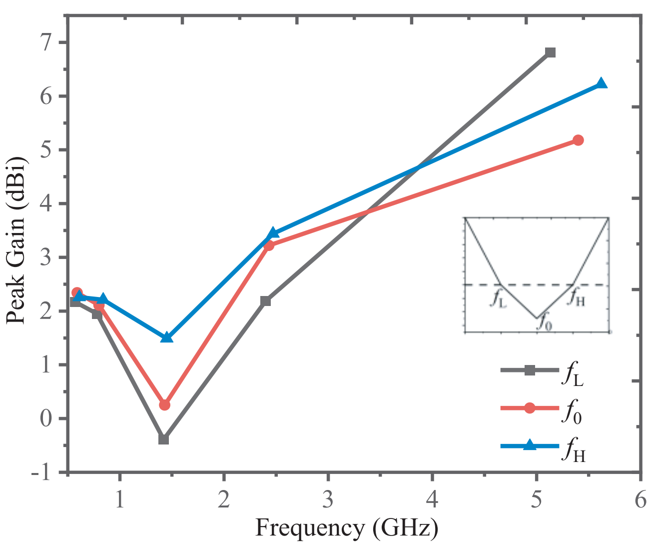

FIGURE 11. Peak gain at start frequency f_L, center frequency f_0, and cut-off frequency f_H.

orates. At the same time, the frequency band of the antenna increases because the antenna excites more modes (3–6 GHz). Therefore, the distance between the branches is an important factor affecting the excitation of the antenna mode in the high-frequency band.

As shown in Figure 1(d), a reverse branch is loaded at end of the longest branch of Ant. 3 in order to expand the bandwidth. The performance after loading is shown in Figure 6. The 1.4 GHz impedance matching performance of the antenna is improved, and the bandwidth is increased after this branch is loaded. The length of the added branch is 34 mm, which corresponds to 1/4 wavelength of 1.4 GHz. This is also the length of the middle branch. With multiple resonant branches working together, the antenna bandwidth reaches the target requirement.

Based on the previous work, the spacing is further reduced to obtain Ant. 5. This is shown in Figure 7(a). Decreasing the distance d between branches, the bandwidth (5–6 GHz) of Ant. 4 is continuously expanded. When d is 1.6 mm, the antenna covers the target band. As shown in Figure 7(b), comparing the bandwidths of Ant. 3, 4, and 5, Ant. 5 has the best performance.

TABLE 1. Parameter value of Ant. 5 (unit: mm).

L	W	L1	W1	L2
200	12.8	92	2	69.5
L3	L4	W0	Lr	Wr
36	37	5	34	1
d	dk	d2	h	
1.6	6	2	0.8	

TABLE 2. Comparison of design antennas with other multi-band antennas.

Reference	Antenna Size (mm^2)	Electrical Size	Bandwidth (GHz)	Covered band
[8]	300×16	$2.4\lambda \times 0.128\lambda$	2.33–2.62	WLAN
[21]	50×50	$0.38\lambda \times 0.38\lambda$	2.51–2.68 3.40–3.60 4.80–4.90	5G NR
[22]	25×20	$0.20\lambda \times 0.16\lambda$	1.85–2.70 3.24–3.99 4.65–5.80	5G NR 4G WiFi/WiMAX
This antenna	200×18	$0.41\lambda \times 0.04\lambda$	0.58–0.60 0.81–0.84 1.41–1.44 2.40–2.52 5.15–5.60	4G LTE WLAN WiFi

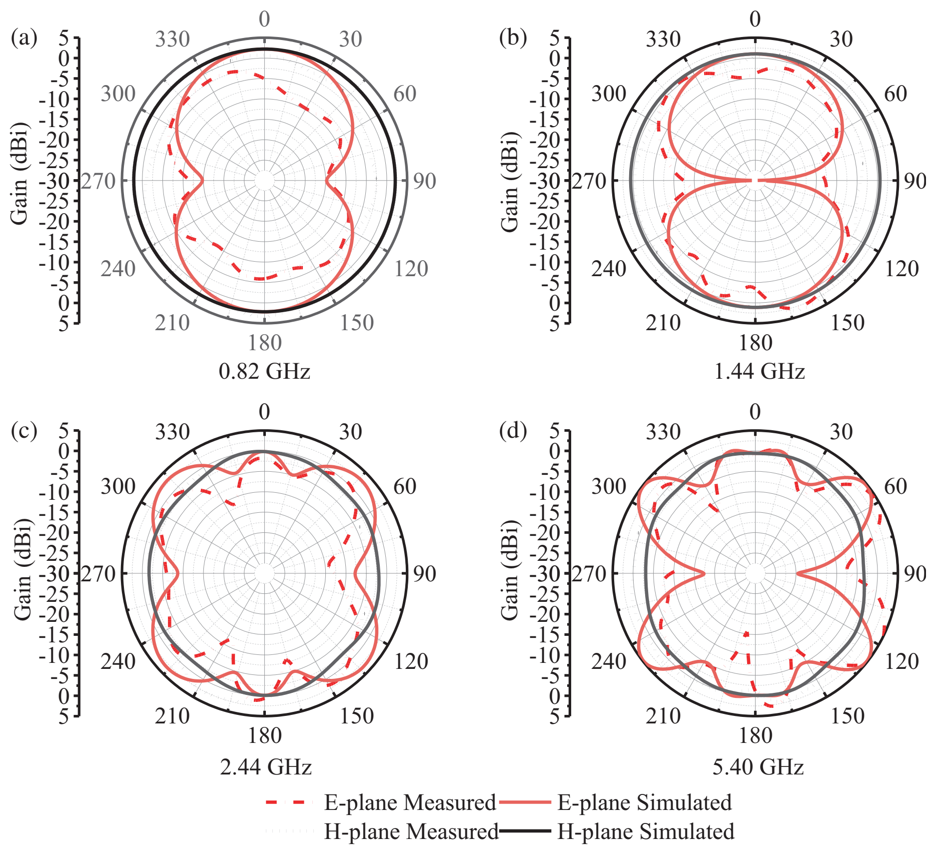

FIGURE 12. Antenna radiation pattern.

The overall view of Ant. 5 is shown in Figure 1(e). The antenna can be divided into two layers: the top radiating surface and dielectric substrate. The dipole antenna has four branches in each arm, and a reverse parasitic branch is added at end of the longest branch. The dielectric substrate material is FR4, and the height is 0.8 mm. The optimized antenna size is shown in Table 1.

In order to better analyze the operation of Ant. 5, the current distribution is provided at five center frequencies. From Figures 8(a)–(c), it can be seen that the maximum current intensity of the antenna at 0.59 GHz occurs at the longest branch. The maximum current strength of the antenna at 0.80 GHz occurs at the next longest branch.

The maximum current intensity of the antenna at 1.43 GHz occurs at the middle two branches and the end loaded reverse branches. At the same time, a strong coupling is generated between the branches. From Figures 8(d) and (e), it can be seen that the antenna has current zeros at the longest or second-longest branches at 2.44 GHz and 5.40 GHz, which is a manifestation of the high harmonics.

3. SIMULATED AND MEASURED RESULTS

In order to experimentally verify the simulation results of the antenna, a prototype of the antenna (Figure 9) was fabricated and tested using a vector network analyzer (PNA-X N5242A). The simulated and measured results of Ant. 5 are shown in Figure 10. The test results of Ant. 5 are in good agreement with simulation ones, and the antenna covers 580–600 MHz, 810–840 MHz, 1410–1440 MHz, 2400–2512 MHz, and 5115–6000 MHz. There is a slight change in the frequency band due to processing and measurement errors. Ant. 5 can work in the expected five frequency bands and can cover the emergency communication band, LTE band, and WLAN/WiFi band. As shown in Figure 11, the gain at each center frequency is greater than 0 dBi. The radiation pattern of the antenna is shown in Figure 12, and the antenna has good horizontal isotropy at the four center frequencies. The gain in the direction of the E and H planes of the antenna is less than 5 dBi.

The antenna proposed in [8] has the characteristics of compact size. The antennas designed in [21, 22] have good multiband characteristics. These characteristics are compared to the antenna designed in this paper, as shown in Table 2. As can be seen from the table, the designed antenna has certain advantages in most frequency bands, relatively small size, and simple structure.

4. CONCLUSION

In this paper, a novel dipole structure is proposed, which helps the antenna to achieve multi-frequency performance, covering five frequency bands required for communication in underground mine environment. The antenna has a small size of $0.41\lambda \times 0.04\lambda$, where λ is the wavelength of the lowest operating frequency 0.59 GHz. The antenna is first designed at normal size based on the multi-branch methods and high harmonics. Branches corresponding to 0.6, 0.8, and 1.4 GHz are designed to cover all the target bands. Then, the antenna size was adjusted to meet the requirements. The 1.4 GHz band was expanded by adding middle branches and loading the reverse branch at end of the longest branch. The high frequency performance of the antenna is optimized by adjusting the spacing. The designed antenna has the advantages of multiband, small size, low cost, and easy integration, which is of great significance for the application and research of multiband antennas for mining.

ACKNOWLEDGEMENT

This work was supported by the Open Fund Project of State Key Laboratory of Gas Disaster Monitoring and Emergency Technology (2022SKLKF12).

REFERENCES

[1] Zhang, H., B. Li, M. Karimi, S. Saydam, and M. Hassan, "Recent advancements in IoT implementation for environmental, safety, and production monitoring in underground mines," *IEEE Internet of Things Journal*, Vol. 10, No. 16, 14 507–14 526, 2023.

[2] Reddy, S. K., A. S. Naik, and G. R. Mandela, "Development of a novel real-time environmental parameters monitoring system based on the internet of things with LoRa modules in underground mines," *Wireless Personal Communications*, Vol. 133, No. 3, 1517–1546, 2023.

[3] Stoicuta, O., S. Riurean, S. Burian, M. Leba, and A. Ionica, "Application of optical communication for an enhanced health and safety system in underground mine," *Sensors*, Vol. 23, No. 2, 692, 2023.

[4] Bazargur, B., O. Bataa, and U. Budjav, "Reliability study for communication system: A case study of an underground mine," *Applied Sciences*, Vol. 13, No. 2, 821, 2023.

[5] Javaid, F., A. Wang, M. U. Sana, A. Husain, and I. Ashraf, "Characteristic study of visible light communication and influence of coal dust particles in underground coal mines," *Electronics*, Vol. 10, No. 8, 883, 2021.

[6] RayChowdhury, A., A. Pramanik, and G. C. Roy, "New approach for localization and smart data transmission inside underground mine environment," *SN Applied Sciences*, Vol. 3, No. 6, 604, 2021.

[7] Yan, Y. and W. Cao, "The mining method of anti-electromagnetic interference for electronic equipment in coal mine by considering network communication technology," *Microelectronics Journal*, Vol. 109, 104987, 2021.

[8] Dong, P., Y. Xu, N. Li, and S. Li, "Design of a tri-band MIMO antenna with high isolation for coal mine wireless communication," in *2023 IEEE MTT-S International Microwave Workshop Series on Advanced Materials and Processes for RF and THz Applications (IMWS-AMP)*, 1–3, Chengdu, China, 2023.

[9] Xu, Y., Z. Zhang, A. Wang, and J. Hou, "Design of three multibranch microstrip antennas compatible with WiMAX/WiFi/4G/5G NR for coal mine applications," *Microwave and Optical Technology Letters*, Vol. 65, No. 3, 892–900, 2023.

[10] Aminu-Baba, M., M. K. A. Rahim, F. Zubir, A. Y. Iliyasu, K. I. Jahun, M. F. M. Yusoff, M. M. Gajibo, A. A. Pramudita, and I. K. C. Lin, "A compact triband miniaturized MIMO antenna for WLAN applications," *AEU — International Journal of Electronics and Communications*, Vol. 136, 153767, 2021.

[11] Yang, G., S. Zhang, J. Li, Y. Zhang, and G. F. Pedersen, "A multiband magneto-electric dipole antenna with wide beam-width," *IEEE Access*, Vol. 8, 68 820–68 827, 2020.

[12] Wang, N., Y. Gao, and Q. Zeng, "Compact wideband omnidirectional UHF antenna for TV white space cognitive radio application," *AEU — International Journal of Electronics and Communications*, Vol. 74, 158–162, 2017.

[13] Ichinose, M., K. Matsubayashi, N. Michishita, and H. Morishita, "Study on broadband sleeve antenna with plate element and parasitic element," in *2020 International Workshop on Antenna Technology (iWAT)*, 1–2, Bucharest, Romania, 2020.

[14] Song, X., G. Zhang, and C. Zhou, "A RT-FDTD method of analyzing wireless propagation characteristics in underground mine," *Scientific Reports*, Vol. 14, No. 1, 9756, 2024.

[15] Song, C., Y. Huo, X. Zhao, W. Gao, W. Cheng, Y. Sun, and Q. Hu, "Analysis of time delay characteristics of mine roadway based on multi-mode theory," in *2022 IEEE 14th International Conference on Advanced Infocomm Technology (ICAIT)*, 55–59, Chongqing, China, 2022.

[16] Gangwar, K., G. C.-Y. Chen, K. K.-M. Chan, R. K. Gangwar, and K. Rambabu, "Antenna system for communication in underground mining environment to ensure miners safety," *IEEE Access*, Vol. 9, 150 162–150 171, 2021.

[17] Huo, Y., L. Zhao, Q. Hu, E. Ding, X. Zhao, and Z. Sun, "Optimal deployment of antenna for field coverage in coal mine tunnels," *IEEE Access*, Vol. 8, 51 954–51 963, 2020.

[18] Huo, Y., Q. Hu, Y. Sun, X. Guo, L. Qi, X. Zhao, and E. Ding, "Optimization of wireless communication coverage in underground tunnels based on zone division," *International Journal of Antennas and Propagation*, Vol. 2020, No. 1, 8826546, 2020.

[19] Sun, J., "Research and development of 5G communication system standards for coal mines," *Journal of Mine Automation*, Vol. 49, 1–8, 2023.

[20] Sun, J., W. Liang, M. Peng, *et al.*, "Analysis and testing of wireless transmission attenuation in coal mine underground and research on the optimal operating frequency band," *Journal of Mine Automation*, Vol. 49, 1–8, 2023.

[21] Xu, Y., T. Bai, Z. Zhang, A. Wang, C. Cui, and J. Hou, "A compact multi-band monopole antenna for 5G NR coal mine applications," *Progress in Electromagnetics Research Letters*, Vol. 115, 57–62, 2024.

[22] Xu, Y., P. Dong, A. Wang, J. Hou, and S. Li, "A quad-band high-isolated MIMO microstrip antenna for coal mine communication," *Progress In Electromagnetics Research Letters*, Vol. 115, 39–46, 2024.